

<https://helda.helsinki.fi>

---

## Unwanted Indoor Air Quality Effects from Using Ultraviolet C Lamps for Disinfection

Graeffe, Frans

2023-01-13

---

Graeffe , F , Luo , Y , Guo , Y & Ehn , M 2023 , ' Unwanted Indoor Air Quality Effects from Using Ultraviolet C Lamps for Disinfection ' , Environmental Science & Technology Letters , vol. 10 , no. 2 , pp. 172-178 . <https://doi.org/10.1021/acs.estlett.2c00807>

---

<http://hdl.handle.net/10138/354661>

<https://doi.org/10.1021/acs.estlett.2c00807>

---

cc\_by

publishedVersion

---

*Downloaded from Helda, University of Helsinki institutional repository.*

*This is an electronic reprint of the original article.*

*This reprint may differ from the original in pagination and typographic detail.*

*Please cite the original version.*

# Unwanted Indoor Air Quality Effects from Using Ultraviolet C Lamps for Disinfection

Frans Graeffe,\* Yuanyuan Luo, Yishuo Guo, and Mikael Ehn\*



Cite This: *Environ. Sci. Technol. Lett.* 2023, 10, 172–178



Read Online

ACCESS |



Metrics & More



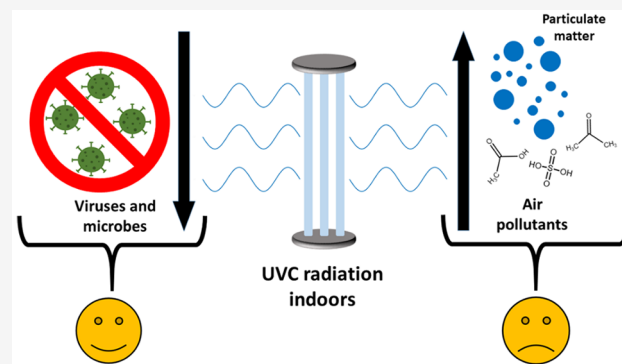
Article Recommendations



Supporting Information

**ABSTRACT:** Ultraviolet germicidal irradiation (UVGI) is known to inactivate various viruses and bacteria, including SARS-CoV-2, and is widely applied especially in medical facilities. This inactivation results from the high photon energies causing molecular bonds to break, but when nonpathogen molecules are affected, unwanted effects may occur. Here, we explored the effect of a commercial high-intensity (~2 kW) UVC disinfection device on the composition and concentration of gases and particles in indoor air. We find that the UVC (254 nm) caused dramatic increases in particle number concentrations, and nearly all (~1000) monitored gas phase species also increased. These responses were unsurprising when considering the typical impacts of UVC on atmospheric chemistry. High particle concentrations are associated with adverse health effects, suggesting that the impact of UVGI devices on indoor air quality (IAQ) should be studied in much more detail. The high-intensity device in this study was intended for short durations in unoccupied rooms, but lower-intensity devices for continuous use in occupied rooms are also widely applied. This makes further studies even more urgent, as the potential IAQ effects of these approaches remain largely unexplored.

**KEYWORDS:** indoor air quality, disinfection, air cleaning, secondary chemistry, UVGI, air pollutants



## INTRODUCTION

In the wake of the COVID-19 pandemic, there has been increasing interest for methods to slow the spread of the virus. Ultraviolet germicidal irradiation (UVGI),<sup>1</sup> which uses ultraviolet C (UVC) radiation to inactivate bacteria and viruses, has been used to photosterilize air and surfaces in hospitals already for decades.<sup>2–4</sup> Several UVC disinfection devices have been developed<sup>5–9</sup> with additional potential applications in e.g. offices and warehouses. SARS-CoV-2 is primarily transmitted by airborne means,<sup>10,11</sup> and since it is inactivated by UVC,<sup>12–15</sup> interest in UVGI devices has seen an upswing during the pandemic. As direct UVC radiation exposure is harmful to humans and can cause e.g. erythema and photokeratitis,<sup>1,16–18</sup> overexposure of UVC radiation should be avoided. However, low intensity UVGI devices, installed in the upper part of rooms (upper-room UV), have been used already for decades for occupied rooms to prevent the spread of diseases.<sup>4,19,20</sup> Recently, UVC devices with wavelengths around 222 nm have been suggested as viable also in occupied rooms, as this wavelength might have more limited health effects,<sup>21–24</sup> but this topic remains debatable.<sup>25,26</sup> In all cases, the efficiency of disinfection will depend on irradiation volume, intensity, and time.

In the atmosphere, the photolyzing ability, i.e. ability to break molecular bonds, of solar UV radiation initializes the

majority of the chemistry taking place in the air,<sup>27,28</sup> including the formation of oxidants, e.g. ozone and the gas phase hydroxyl (OH) radical. Both photolysis of, and radical reactions with, volatile gases and compounds emitted from surface materials<sup>29,30</sup> can form new compounds, with different properties concerning e.g. toxicity or volatility. Less volatile compounds can contribute to aerosol formation. These unwanted gas- and particle-phase compounds can have adverse human health effects,<sup>31–33</sup> raising concerns about using UVC radiation from the indoor air quality (IAQ) perspective.

In this study, we attempted to characterize the production of gaseous and particulate components when using a commercial, high-intensity UVC device, to determine whether potentially negative IAQ impacts can be expected. Utilizing state-of-the-art mass spectrometers and an ozone monitor we measured gas phase compounds while simultaneously sampling aerosol particle number and size distributions produced from the UVC light exposure.

**Received:** November 1, 2022

**Revised:** January 10, 2023

**Accepted:** January 10, 2023

**Published:** January 13, 2023



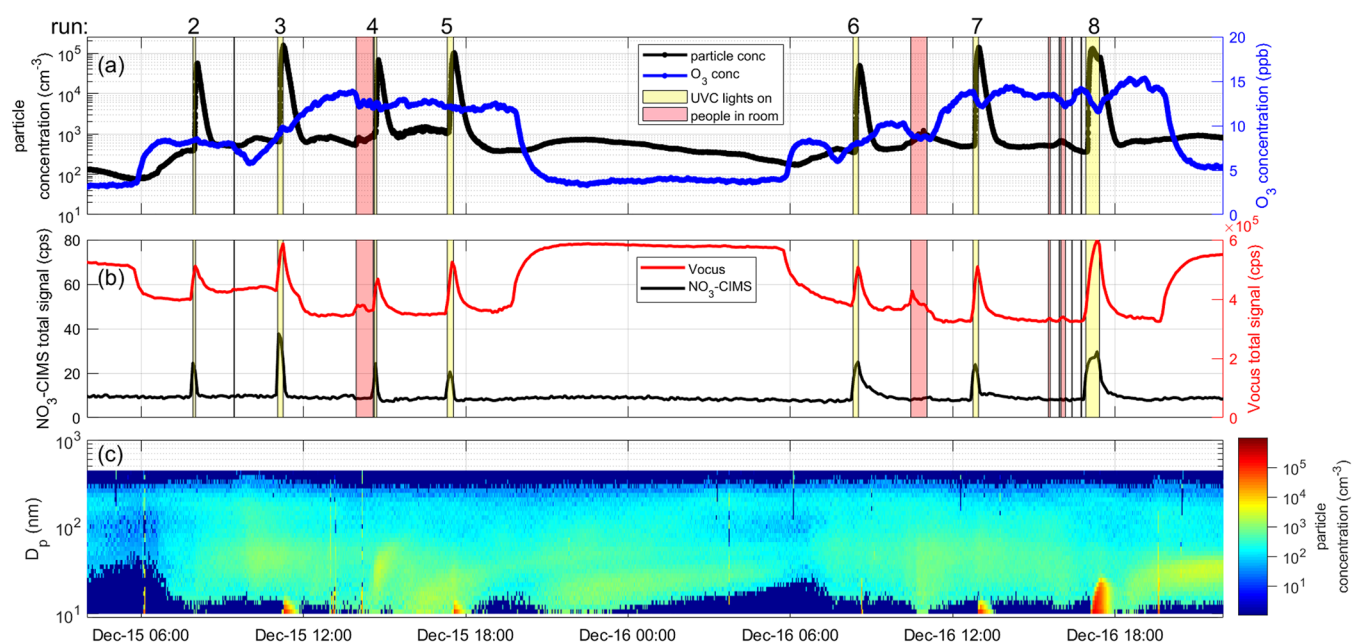


**Figure 1.** Time series of particle number and O<sub>3</sub> concentrations (a), NO<sub>3</sub>-CIMS and Vocus total signal (b), and particle number size distribution (c) during the UVC irradiation experiments (runs 2–8). The yellow highlighted area is when the UVC lights were on, and the red highlighted area is when people were in the room. At the top of the figure, the run number for each UVC irradiation experiment is mentioned (see Table S1). Time series of all runs (1–14) and daily time series of each day are presented in the SI (Figures S3–S7).

## MATERIAL AND METHODS

We used a hospital-grade SteriPro-UVGI device designed for fast disinfection in large rooms, e.g. operating rooms (by UVC Solutions<sup>34</sup>), and it has 16 Philips Hg TUV 95 W and 8 Philips Hg TUV 60 W lamps, emitting at a peak wavelength of 254 nm, and minor emissions at higher wavelengths. Hg UV lamps also produce 185 nm UV light, which forms O<sub>3</sub> from O<sub>2</sub> photolysis, but these wavelengths should be filtered out by the device. A more detailed description of the device is provided in the Supporting Information (SI) Text S1.

All experiments were conducted in an aerosol physics laboratory (~30 m<sup>2</sup> and ~110 m<sup>3</sup>) at the University of Helsinki. Temperature and RH varied between 26.6 and 28.6 °C and 15%–21%, respectively. The ozone concentrations were relatively low (2–15 ppb), with the main source being transported from outside through the ventilation system and sinks being both outward ventilation and reactions in the room. During the experiments, outside ozone levels were unusually low and, therefore in 3 out of 14 experiments (Table S1), were increased slightly by using an ozone generator. The HVAC system (Heating, Ventilating, and Air Conditioning) in the laboratory was a single pass design where the outdoor air was filtered and heated before entering the room and then directly exhausted without any recirculating. The ventilation rate was ~4.2 ACH (air changes per hour) during the daytime, as determined from CO<sub>2</sub> decay experiments (Figure S17), and ~2.8 ACH during the night.

The unoccupied laboratory was irradiated for a given duration: 6 (recommended), 12, or 30 min. We also tested 4 times 6 min consecutively with only 10 min intervals (runs 11–14). As these are less comparable to other experiments, they are omitted from calculations unless otherwise noted. After the UVGI device shutdown, we waited at least 75 min before entering the room. To test the effect of human emissions on the air chemistry, we conducted experiments both with and without people's presence prior to the

disinfection cycle. The room air was continuously sampled with several instruments to monitor changes in the composition of gases and particles. We used two chemical ionization mass spectrometers: a Vocus PTR<sup>35</sup> for volatile organic compounds (VOCs) and a nitrate (NO<sub>3</sub><sup>-</sup>) based CI-API-TOF<sup>36</sup> (hereafter NO<sub>3</sub>-CIMS) for the most oxygenated compounds. Ozone was monitored with a Thermo Scientific Model 49i Analyzer. Aerosol particle number concentration was measured with a Condensation Particle Counter (CPC, TSI model 3788, lower detection limit of 2.5 nm), and the aerosol size distribution was measured with a scanning mobility particle sizer (SMPS, 10 nm–500 nm). Aerosol bulk composition was measured using an Aerosol Mass Spectrometer (LToF-AMS).<sup>37</sup> More details of the instruments are provided in the SI.

## RESULTS

When the UVC lights were turned on, dramatic changes were observed in nearly all monitored parameters (Figure 1). First, we present particle phase results, followed by gas phase results.

**Particle Formation.** Time series of particle number concentration (Figure 1a) and size distribution (Figure 1c) clearly show that a high concentration of small particles is formed whenever the UVC lights were turned on. Formation rates (Table S1) of 2.5 nm particles were determined to be 250 particles cm<sup>-3</sup> s<sup>-1</sup> (median), increasing the particle number concentrations from background levels of <1000 cm<sup>-3</sup> to between 4.5·10<sup>4</sup> cm<sup>-3</sup> and 1.6·10<sup>5</sup> cm<sup>-3</sup>, depending on the irradiation time and ozone concentration (Figure S1). Once the lamps were turned off, particle concentrations rapidly decayed with a median *e*-folding time of 6.2 min (corresponding to ~10 ACH), suggesting that the particle decrease was due not only to ventilation but also to surface deposition and coagulation. In the experiments with longer irradiation times, the particle concentrations started to stabilize during irradiation, with formation balanced with coagulation loss

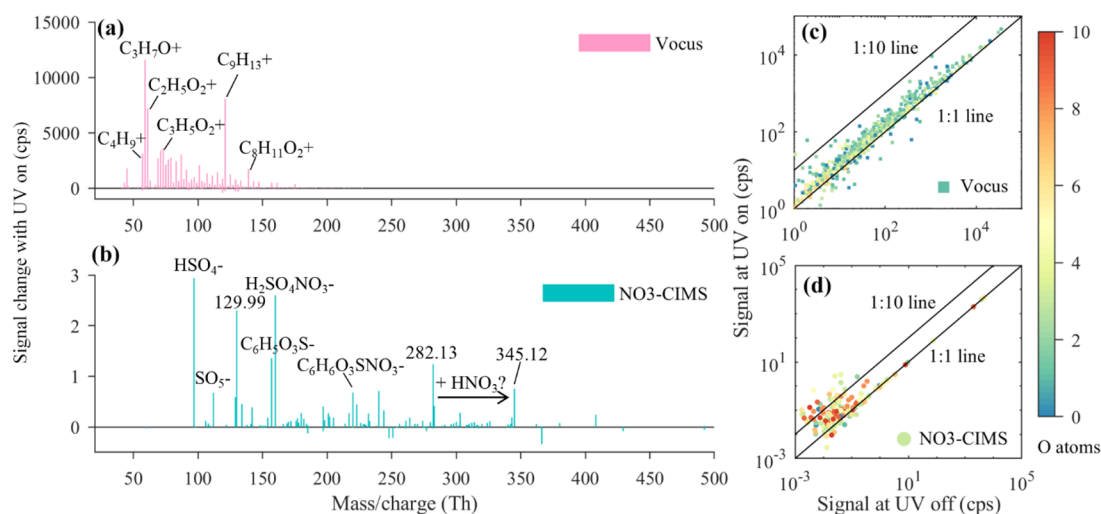


**Figure 2.** Changes in gas phase composition from a single UVC irradiation run (run 7). Panels (a) and (b) show difference mass spectra between periods with UVC on and UVC off for the Vocus and NO<sub>3</sub>-CIMS, respectively. Reagent ions and water clusters were removed from the mass spectra. Unidentified compounds in panel (b) are labeled with their mass-to-charge ratios. Relative signal intensity changes for species detected by Vocus and NO<sub>3</sub>-CIMS are plotted in panels (c) and (d), respectively. The color scale indicates the O atom content in the identified species.

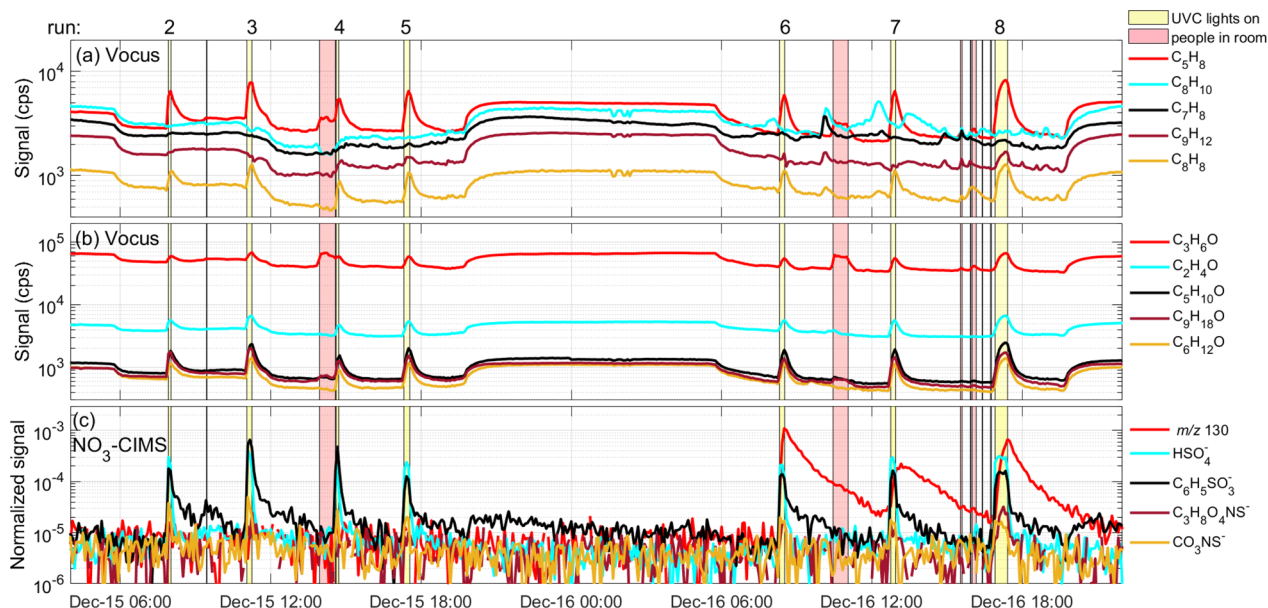


**Figure 3.** Time variations of selected gas-phase compounds measured by Vocus and NO<sub>3</sub>-CIMS during the UVC irradiation experiments (runs 2–8). Hydrocarbon (including some presumably aromatic and isoprene) VOCs (a) and oxygenated VOCs (b) were measured by Vocus, and sulfur-containing compounds and one unidentified compound (*m/z* 130) (c) were measured by NO<sub>3</sub>-CIMS. The yellow and red shaded areas are when the UVC lights were turned on and when people were in the room, respectively. At the top of the figure, the run number for each UVC irradiation experiment is mentioned (see Table S1). The charging H<sup>+</sup> adduct is removed from all Vocus-measured compounds in the legend. Time variation of all runs (1–14) is presented in the SI (Figure S14).

and ventilation (Figure S2). There was no noticeable increase in particle mass concentration, as the newly formed particles did not grow above 30 nm in size. No significant difference in the particle concentrations was observed whether or not people were in the laboratory before the disinfection cycle.

**Ozone.** The indoor ozone concentrations were generally low and tracked outdoor concentrations (Figures 1a, S8–S9) but were lower due to reactions with indoor VOCs and surfaces. At night (~19:30–5:30), the HVAC was automatically decreased, leading to longer indoor residence times and increased VOCs (see below), further lowering the ozone concentrations compared to outdoors. 254 nm UVC is known

to photolyze ozone, forming gas phase OH radicals (a typical method of initiating oxidation and aerosol formation in atmospheric simulation chambers),<sup>38,39</sup> and therefore, we would expect O<sub>3</sub> decreases when lights were on. Our data indicate not only that changes in ozone were overall small but also that some ozone production may take place. This could be due to either O<sub>2</sub> photolysis from minor leaking of 185 nm radiation or from NO<sub>2</sub> (originating from outdoor air, Figure S8b) photolysis by wavelengths > 254 nm (A violet glow was visible).<sup>40</sup> We cannot quantify either process and can thus only suggest that such processes also be kept in mind. See also Figure S10 and the related discussion.

**VOCs.** Vocus total signal always increased when the UVC device was turned on, as well as during nights when the HVAC was decreased (Figure 1b). As shown in Figures 2a and 2c, the levels of almost all individual compounds increased, which was surprising as we expected many of the VOCs to decrease following direct photolysis or reactions with gas phase OH. The top-15 compounds with the highest signal increase are summarized in Table S2, topped by C<sub>3</sub>H<sub>6</sub>O (acetone), C<sub>8</sub>H<sub>8</sub>O (potentially phenylacetaldehyde), and C<sub>2</sub>H<sub>4</sub>O<sub>2</sub> (acetic acid).

The temporal variations of some selected hydrocarbon VOCs and oxygenated organic compounds are shown in Figures 3a–3b. Figures S11 and S12 show the behavior of the same compounds in a single run (run 8). These have sources from building materials, such as gypsum, paint, vinyl flooring, and linoleum.<sup>41,42</sup> Isoprene and acetone concentrations increased significantly when people entered the laboratory, consistent with studies of human-derived emissions.<sup>43</sup> We also found that the mass spectrum produced during UVC irradiation was very similar to that during nights with lowered HVAC (Figure S13), leading us to hypothesize that the UVC caused enhanced evaporation from surfaces. We cannot determine the exact cause of this, but the room air temperature (data not logged) barely changed during irradiation (within 1 °C). Therefore, we speculate that the energy from the radiation might be absorbed by molecules on surfaces and an increase in their thermal energy leading to increased evaporation.

**Oxidation Products.** Similar to the Vocus, there is a dramatic increase in the total signal of the NO<sub>3</sub>–CIMS (Figure 1b) whenever the UVC lights were turned on, and the increase concerns nearly all measured signals (Figures 2b and 2d). The NO<sub>3</sub>–CIMS mass spectrum consists mainly of inorganic acids, highly oxygenated organic molecules (HOMs)<sup>44,45</sup> with up to ten oxygen atoms, and organosulfur compounds. The increase of these oxidation products is most likely due to high gas phase OH radical concentrations that react with compounds in the air or on surfaces. In addition, ozonolysis plays an important role in oxidizing the organic compounds. HOMs and H<sub>2</sub>SO<sub>4</sub> are known to be some of the most efficient particle-forming compounds in the atmosphere<sup>46,47</sup> due to their low volatilities, explaining the fast increase in the particle number concentrations. As the NO<sub>3</sub>–CIMS is mainly selective toward low-volatile species, no significant differences were detected from volatile species evaporating from people entering the laboratory or when the HVAC decreased at nights (Figure S15).

Figure 3c (and Figure S16 for run 8) shows the temporal trends of five different compounds with obvious increases with UVC irradiation. In addition to sulfuric acid vapors (HSO<sub>4</sub><sup>−</sup> and H<sub>2</sub>SO<sub>4</sub>·NO<sub>3</sub><sup>−</sup>, Figure 2b), formed from gas phase OH oxidation of SO<sub>2</sub>, we also detected several S-containing organic compounds with one to nine carbon atoms. The main signals were C<sub>6</sub>H<sub>6</sub>O<sub>3</sub>S, CHNO<sub>3</sub>S, and C<sub>3</sub>H<sub>8</sub>OS. The molecular structures remain unknown, but we speculate that C<sub>6</sub>H<sub>6</sub>O<sub>3</sub>S can correspond to benzenesulfonic acid. These and other potentially undetected, S-containing species may explain the smell we noticed when entering the laboratory after the UVC irradiation, which is typically observed after UVGI disinfection, according to discussion with hospital personnel operating a similar device. Finally, a compound at *m/z* 130 became one of the most dominant peaks in the NO<sub>3</sub>–CIMS mass spectra from run 6 onward (Figure 3c). Our best guess for the composition based on the exact mass and isotope ratios is

H<sub>5</sub>O<sub>5</sub>N<sub>1</sub>P<sub>1</sub><sup>−</sup>. Organophosphorus compounds have been increasingly applied as flame retardants,<sup>48,49</sup> but we cannot associate this with any expected molecules; therefore, this assignment remains purely tentative.

## DISCUSSION AND CONCLUSIONS

UVGI devices efficiently deactivate pathogens, but our findings suggest that the UVC radiation can greatly affect the indoor air chemistry, consequently producing unwanted particles and gas phase compounds. The ultimate impacts on IAQ from UVGI are likely highly dependent on the intensity and duration of the irradiation, along with the ozone concentration and available VOCs in the room. The device tested in this study was high-intensity, designed for short durations, and the effects on the air compositions were therefore significant. We had a ventilation rate of ~4.2 ACH in our laboratory, and it took ~30–40 min for particle concentrations to reach pre-UVGI levels. As such, entering the room directly after UVGI disinfection, still with high particle and gas phase concentrations, on a regular basis may be a potential health risk. For the above reasons, these effects should be studied in more detail, under different conditions, with different types of devices. To our knowledge, the observed enhanced evaporation from surfaces due to UVC light remains a completely unstudied effect from an IAQ perspective.

The HVAC system has a crucial role for decreasing the contaminant concentrations after, and during, the UVC irradiation. By increasing the ventilation rate, the concentration of UVGI-produced air pollutants would decrease faster, but a more effective HVAC system would by itself reduce airborne (virus) particles, making the UVGI disinfection less required. Another place-dependent factor that was not studied here was the levels of air pollutants in the room prior to the UVGI procedure, e.g. how efficiently the HVAC system filtered potential polluted outdoor air. If the particle loadings in the room are already high, the UVGI-initiated gas phase compounds might not form new particles but instead condense onto already existing particles. As the deposition of particles in different parts of the human respiratory tract is dependent on the particle size,<sup>50</sup> with small particles penetrating deeper (increasing deposition with decreasing particle size from 200 to 10 nm), the particle size distribution is important. As particle formation is a highly nonlinear process,<sup>51</sup> we do not expect that our results (neither particle nor gas phase) can be quantitatively extrapolated to any other UVGI devices or conditions.

The UVC power per unit area and volume in our study was 2000 W/30 m<sup>2</sup> = 67 Wm<sup>−2</sup> and 2000 W/110 m<sup>3</sup> = 18 Wm<sup>−3</sup>, respectively. These values are clearly higher than some existing guidelines for upper-room UV installations,<sup>52,53</sup> 1.7 W m<sup>−2</sup> or 6 W m<sup>−3</sup> (With a room height of 2.8 m, this corresponds to 17 W m<sup>−2</sup>). However, upper-room UV devices are active for longer times (hours), while the UVC device in this study had a significantly shorter recommended irradiation time (6 min). Thus, the radiation is more intense, but the total irradiation should be similar when averaging over a day.

Different methods have been applied or suggested to avoid the problem of overexposure or direct irradiation of harmful UVC light, including the commonly used upper-room UV or placing UVC lamps inside HVAC systems.<sup>54,55</sup> Using “far-UVC” devices, with wavelengths around 222 nm, and whether they are safe or not, is still under debate. In all cases, the effects on air chemistry may still be analogous to those observed in

our study, leading to worsened IAQ. Furthermore, UVGI devices developed mainly for household use,<sup>56</sup> where air exchange rates can be very low, also possess potential problems for IAQ. As already discussed in Joo et al. (2021)<sup>57</sup> and Collins and Farmer (2021),<sup>33</sup> the impacts of different air and surface cleaning technologies to secondary chemistry need to be acknowledged and should be urgently studied from the perspective of adverse health effects before becoming widely applied in various indoor environments.

## ■ ASSOCIATED CONTENT

### SI Supporting Information

The Supporting Information is available free of charge at <https://pubs.acs.org/doi/10.1021/acs.estlett.2c00807>.

UVGI device and its operation (Text S1); description of Vocus and NO<sub>3</sub>-CIMS operation (Text S2); maximum particle concentration (from CPC) versus UVC exposure time (Figure S1); particle concentrations during run 8 with fitted functions for calculation of FR and *e*-folding time (Figure S2); time series of whole experiment and individual days for particle number and O<sub>3</sub> concentrations and NO<sub>3</sub>-CIMS and Vocus total signal and particle number size distribution (Figures S3–S7); time series of indoor and ambient O<sub>3</sub> concentrations and ambient NO and NO<sub>x</sub> concentrations (Figure S8); indoor vs ambient O<sub>3</sub> concentrations (Figure S9); impact on indoor ozone concentration during UVC irradiation (Figure S10); response of 10 different compounds measured by Vocus during run 8 (Figures S11–S12); Vocus signals of UV<sub>On-Off</sub> vs Night-UV<sub>Off</sub> (Figure S13); time series of selected compounds measured by NO<sub>3</sub>-CIMS and Vocus for runs 1–14 (Figure S14); NO<sub>3</sub>-CIMS signals of UV<sub>On-Off</sub> vs Night-UV<sub>Off</sub> (Figure S15); response of 10 different compounds measured by NO<sub>3</sub>-CIMS during run 8 (Figure S16); CO<sub>2</sub> measurements for estimating air exchange rate in laboratory (Figure S17); UVC irradiation experiments with individual run number information (Table S1); and top-15 compounds according to increase of signal intensity measured by Vocus during run 8 (Table S2) (PDF)

## ■ AUTHOR INFORMATION

### Corresponding Authors

**Frans Graeffe** – Institute for Atmospheric and Earth System Research/Physics, Faculty of Science, University of Helsinki, Helsinki 00014, Finland; [orcid.org/0000-0001-7304-4651](https://orcid.org/0000-0001-7304-4651); Email: [frans.graeffe@helsinki.fi](mailto:frans.graeffe@helsinki.fi)

**Mikael Ehn** – Institute for Atmospheric and Earth System Research/Physics, Faculty of Science, University of Helsinki, Helsinki 00014, Finland; [orcid.org/0000-0002-0215-4893](https://orcid.org/0000-0002-0215-4893); Email: [mikael.ehn@helsinki.fi](mailto:mikael.ehn@helsinki.fi)

### Authors

**Yuan Yuan Luo** – Institute for Atmospheric and Earth System Research/Physics, Faculty of Science, University of Helsinki, Helsinki 00014, Finland; [orcid.org/0000-0003-4253-3596](https://orcid.org/0000-0003-4253-3596)

**Yishuo Guo** – Institute for Atmospheric and Earth System Research/Physics, Faculty of Science, University of Helsinki, Helsinki 00014, Finland; Beijing Advanced Innovation

Center for Soft Matter Science and Engineering, Beijing University of Chemical Technology, Beijing 100089, China

Complete contact information is available at:

<https://pubs.acs.org/doi/10.1021/acs.estlett.2c00807>

### Author Contributions

M.E. designed the study. F.G. led the experiments with the help of Y.L. and Y.G. F.G., Y.L., and Y.G. analyzed the data. F.G. wrote the original draft. All authors commented on the manuscript.

### Notes

The authors declare no competing financial interest.

## ■ ACKNOWLEDGMENTS

We would like to thank Raimo Alanen at OmaMedical Oy for lending the SteriPro to us during our experiments. This work was supported by the Academy of Finland (grants 317380 and 345982). F.G. was funded by Svenska Kulturfonden (grants 167344 and 177923). Y.L. and Y.G. thank the China Scholarship Council (grants 201906220191 and 202106880024) for financial support.

## ■ REFERENCES

- (1) Kowalski, W. *Ultraviolet Germicidal Irradiation Handbook*; 2009; DOI: 10.1007/978-3-642-01999-9.
- (2) Sharp, D. G. The effects of ultraviolet light on bacteria suspended in air. *J. Bacteriol.* **1940**, 39 (5), 535–547.
- (3) Kraissl, C. J.; Cimiotti, J. G.; Meloney, F. L. Considerations in the use of ultraviolet radiation in operating rooms. *Ann. Surg.* **1940**, 111 (2), 161.
- (4) Wells, W.; Wells, M.; Wilder, T. The environmental control of epidemic contagion. I. An epidemiologic study of radiant disinfection of air in day schools. *Am. J. Hyg.* **1942**, 35, 97–121.
- (5) Stibich, M.; Stachowiak, J.; Tanner, B.; Berkheiser, M.; Moore, L.; Raad, I.; Chemaly, R. F. Evaluation of a Pulsed-Xenon Ultraviolet Room Disinfection Device for Impact on Hospital Operations and Microbial Reduction. *Infect. Control Hosp. Epidemiol.* **2011**, 32 (3), 286–288.
- (6) Guettari, M.; Gharbi, I.; Hamza, S. UVC disinfection robot. *Environ. Sci. Pollut. Res.* **2021**, 28 (30), 40394–40399.
- (7) Ma, Y.; Xi, N.; Xue, Y. X.; Wang, S. Y.; Wang, Q. Y.; Gu, Y. Development of a UVC-based disinfection robot. *Industrial Robot-the International Journal of Robotics Research and Application* **2022**, 49, 913.
- (8) UVD\_Robots. *UVD Robots*; 2022. <https://uvd.blue-ocean-robotics.com/> (accessed 2022-05-18).
- (9) Bluebotics. *Bluebotics*; 2022. <https://bluebotics.com/mini-uvc-disinfection-robot/> (accessed 2022-05-18).
- (10) Greenhalgh, T.; Jimenez, J. L.; Prather, K. A.; Tufekci, Z.; Fisman, D.; Schooley, R. Ten scientific reasons in support of airborne transmission of SARS-CoV-2. *Lancet* **2021**, 397 (10285), 1603–1605.
- (11) Wang, C. C.; Prather, K. A.; Sznitman, J.; Jimenez, J. L.; Lakdawala, S. S.; Tufekci, Z.; Marr, L. C. Airborne transmission of respiratory viruses. *Science* **2021**, 373 (6558), eabd9149.
- (12) Heilingloh, C. S.; Aufderhorst, U. W.; Schipper, L.; Dittmer, U.; Witzke, O.; Yang, D.; Zheng, X.; Sutter, K.; Trilling, M.; Alt, M.; et al. Susceptibility of SARS-CoV-2 to UV irradiation. *Am. J. Infect. Control* **2020**, 48 (10), 1273–1275.
- (13) Inagaki, H.; Saito, A.; Sugiyama, H.; Okabayashi, T.; Fujimoto, S. Rapid inactivation of SARS-CoV-2 with deep-UV LED irradiation. *Emerging Microbes Infect.* **2020**, 9 (1), 1744–1747.
- (14) Sabino, C. P.; Sellera, F. P.; Sales-Medina, D. F.; Machado, R. R. G.; Durigon, E. L.; Freitas, L. H.; Ribeiro, M. S. UV-C (254 nm) lethal doses for SARS-CoV-2. *Photodiagn. Photodyn. Ther.* **2020**, 32, 101995.

- (15) Biasin, M.; Bianco, A.; Pareschi, G.; Cavalleri, A.; Cavatorta, C.; Fenizia, C.; Galli, P.; Lessio, L.; Lualdi, M.; Tombetti, E.; et al. UV-C irradiation is highly effective in inactivating SARS-CoV-2 replication. *Sci. Rep.* **2021**, *11* (1), 6260.
- (16) Brubaehar, J.; Hoffman, R. S. Hazards of ultraviolet lighting used for tuberculosis control. *Chest* **1996**, *109* (2), 582–583.
- (17) Zaffina, S.; Camisa, V.; Lembo, M.; Vinci, M. R.; Tucci, M. G.; Borra, M.; Napolitano, A.; Cannata, V. Accidental Exposure to UV Radiation Produced by Germicidal Lamp: Case Report and Risk Assessment. *Photochem. Photobiol.* **2012**, *88* (4), 1001–1004.
- (18) Sliney, D. Balancing the Risk of Eye Irritation from UV-C with Infection from Bioaerosols. *Photochem. Photobiol.* **2013**, *89* (4), 770–776.
- (19) Wells, W. Air disinfection in day schools. *American Journal of Public Health and the Nations Health* **1943**, *33* (12), 1436–1443.
- (20) Miller, S. L.; Linnes, J.; Luongo, J. Ultraviolet Germicidal Irradiation: Future Directions for Air Disinfection and Building Applications. *Photochem. Photobiol.* **2013**, *89* (4), 777–781.
- (21) Buonanno, M.; Ponnaiya, B.; Welch, D.; Stanislauskas, M.; Randers-Pehrson, G.; Smilenov, L.; Lowy, F. D.; Owens, D. M.; Brenner, D. J. Germicidal Efficacy and Mammalian Skin Safety of 222-nm UV Light. *Radiat. Res.* **2017**, *187* (4), 493–501.
- (22) Yamano, N.; Kunisada, M.; Kaidzu, S.; Sugihara, K.; Nishiaki-Sawada, A.; Ohashi, H.; Yoshioka, A.; Igarashi, T.; Ohira, A.; Tanito, M.; Nishigori, C. Long-term Effects of 222-nm ultraviolet radiation C Sterilizing Lamps on Mice Susceptible to Ultraviolet Radiation. *Photochem. Photobiol.* **2020**, *96* (4), 853–862.
- (23) Eadie, E.; Barnard, I. M. R.; Ibbotson, S. H.; Wood, K. Extreme Exposure to Filtered Far-UVC: A Case Study. *Photochem. Photobiol.* **2021**, *97* (3), 527–531.
- (24) Eadie, E.; Hiwar, W.; Fletcher, L.; Tidswell, E.; O'Mahoney, P.; Buonanno, M.; Welch, D.; Adamson, C. S.; Brenner, D. J.; Noakes, C.; Wood, K. Far-UVC (222 nm) efficiently inactivates an airborne pathogen in a room-sized chamber. *Sci. Rep.* **2022**, *12* (1), 4373.
- (25) Woods, J. A.; Evans, A.; Forbes, P. D.; Coates, P. J.; Gardner, J.; Valentine, R. M.; Ibbotson, S. H.; Ferguson, J.; Fricker, C.; Moseley, H. The effect of 222-nm UVC phototesting on healthy volunteer skin: a pilot study. *Photodermatology Photoimmunology & Photomedicine* **2015**, *31* (3), 159–166.
- (26) Ong, Q.; Wee, W.; Dela Cruz, J.; Teo, J. W. R.; Han, W. P. 222-Nanometer Far-UVC Exposure Results in DNA Damage and Transcriptional Changes to Mammalian Cells. *International Journal of Molecular Sciences* **2022**, *23* (16), 9112.
- (27) Madronich, S.; Flocke, S. The role of solar radiation in atmospheric chemistry. In *Environmental photochemistry*; Springer: 1999; pp 1–26, DOI: 10.1007/978-3-540-69044-3\_1.
- (28) Seinfeld, J. H.; Pandis, S. N. *Atmospheric Chemistry and Physics: From Air Pollution to Climate Change*, 3rd ed.; Wiley: 2016.
- (29) Kauffman, R. E.; Wolf, J. D. Study of the Degradation of Typical HVAC Materials, Filters, and Components Irradiated by UVC Energy-Part III: Manufactured Components. *ASHRAE Trans.* **2013**, *119*, 203.
- (30) Mitxelena-Iribarren, O.; Mondragon, B.; Perez-Lorenzo, E.; Smerdou, C.; Guillen-Grima, F.; Sierra-Garcia, J. E.; Rodriguez-Merino, F.; Arana, S. Evaluation of the degradation of materials by exposure to germicide UV-C light through colorimetry, tensile strength and surface microstructure analyses. *Mater. Today Commun.* **2022**, *31*, 103690.
- (31) Pekkanen, J.; Peters, A.; Hoek, G.; Tiittanen, P.; Brunekreef, B.; de Hartog, J.; Heinrich, J.; Ibaldo-Mulli, A.; Kreyling, W. G.; Lanki, T.; Timonen, K. L.; Vanninen, E. Particulate air pollution and risk of ST-segment depression during repeated submaximal exercise tests among subjects with coronary heart disease - The exposure and risk assessment for fine and ultrafine particles in ambient air (ULTRA) study. *Circulation* **2002**, *106* (8), 933–938.
- (32) Schraufnagel, D. E. The health effects of ultrafine particles. *Exp. Mol. Med.* **2020**, *52* (3), 311–317.
- (33) Collins, D. B.; Farmer, D. K. Unintended Consequences of Air Cleaning Chemistry. *Environ. Sci. Technol.* **2021**, *55* (18), 12172–12179.
- (34) UVC Solutions. *UVC Solutions*; 2022. <https://www.uvc-solutions.com/> (accessed 2022-09-20).
- (35) Krechmer, J.; Lopez-Hilfiker, F.; Koss, A.; Hutterli, M.; Stoermer, C.; Deming, B.; Kimmel, J.; Warneke, C.; Holzinger, R.; Jayne, J.; Worsnop, D.; Fuhrer, K.; Gonin, M.; de Gouw, J. Evaluation of a New Reagent-Ion Source and Focusing Ion–Molecule Reactor for Use in Proton-Transfer-Reaction Mass Spectrometry. *Anal. Chem.* **2018**, *90* (20), 12011–12018.
- (36) Jokinen, T.; Sipila, M.; Junninen, H.; Ehn, M.; Lonn, G.; Hakala, J.; Petaja, T.; Mauldin, R. L.; Kulmala, M.; Worsnop, D. R. Atmospheric sulphuric acid and neutral cluster measurements using CI-API-TOF. *Atmos. Chem. Phys.* **2012**, *12* (9), 4117–4125.
- (37) DeCarlo, P. F.; Kimmel, J. R.; Trimborn, A.; Northway, M. J.; Jayne, J. T.; Aiken, A. C.; Gonin, M.; Fuhrer, K.; Horvath, T.; Docherty, K. S.; Worsnop, D. R.; Jimenez, J. L. Field-deployable, high-resolution, time-of-flight aerosol mass spectrometer. *Anal. Chem.* **2006**, *78* (24), 8281–8289.
- (38) Lambe, A. T.; Chhabra, P. S.; Onasch, T. B.; Brune, W. H.; Hunter, J. F.; Kroll, J. H.; Cummings, M. J.; Brogan, J. F.; Parmar, Y.; Worsnop, D. R.; Kolb, C. E.; Davidovits, P. Effect of oxidant concentration, exposure time, and seed particles on secondary organic aerosol chemical composition and yield. *Atmos. Chem. Phys.* **2015**, *15* (6), 3063–3075.
- (39) Palm, B. B.; Campuzano-Jost, P.; Ortega, A. M.; Day, D. A.; Kaser, L.; Jud, W.; Karl, T.; Hansel, A.; Hunter, J. F.; Cross, E. S.; Kroll, J. H.; Peng, Z.; Brune, W. H.; Jimenez, J. L. In situ secondary organic aerosol formation from ambient pine forest air using an oxidation flow reactor. *Atmos. Chem. Phys.* **2016**, *16* (5), 2943–2970.
- (40) Krupa, S. V.; Manning, W. J. ATMOSPHERIC OZONE - FORMATION AND EFFECTS ON VEGETATION. *Environ. Pollut.* **1988**, *50* (1–2), 101–137.
- (41) Han, K. H.; Zhang, J. S.; Wargocki, P.; Knudsen, H. N.; Guo, B. Determination of material emission signatures by PTR-MS and their correlations with odor assessments by human subjects. *Indoor Air* **2010**, *20* (4), 341–354.
- (42) Rizk, M.; Guo, F. F.; Verrielle, M.; Ward, M.; Dusanter, S.; Blond, N.; Locoge, N.; Schoemaeker, C. Impact of material emissions and sorption of volatile organic compounds on indoor air quality in a low energy building: Field measurements and modeling. *Indoor Air* **2018**, *28* (6), 924–935.
- (43) Liu, S.; Li, R.; Wild, R. J.; Warneke, C.; de Gouw, J. A.; Brown, S. S.; Miller, S. L.; Luongo, J. C.; Jimenez, J. L.; Ziemann, P. J. Contribution of human-related sources to indoor volatile organic compounds in a university classroom. *Indoor Air* **2016**, *26* (6), 925–938.
- (44) Ehn, M.; Thornton, J. A.; Kleist, E.; Sipila, M.; Junninen, H.; Pullinen, I.; Springer, M.; Rubach, F.; Tillmann, R.; Lee, B.; Lopez-Hilfiker, F.; Andres, S.; Acir, I. H.; Rissanen, M.; Jokinen, T.; Schobesberger, S.; Kangasluoma, J.; Kontkanen, J.; Nieminen, T.; Kurten, T.; et al. A large source of low-volatility secondary organic aerosol. *Nature* **2014**, *506* (7489), 476.
- (45) Bianchi, F.; Kurten, T.; Riva, M.; Mohr, C.; Rissanen, M. P.; Roldin, P.; Berndt, T.; Crounse, J. D.; Wennberg, P. O.; Mentel, T. F.; Wildt, J.; Junninen, H.; Jokinen, T.; Kulmala, M.; Worsnop, D. R.; Thornton, J. A.; Donahue, N.; Kjaergaard, H. G.; Ehn, M. Highly Oxygenated Organic Molecules (HOM) from Gas-Phase Autoxidation Involving Peroxy Radicals: A Key Contributor to Atmospheric Aerosol. *Chem. Rev.* **2019**, *119* (6), 3472–3509.
- (46) Petäjä, T.; Mauldin Iii, R.; Kosciuch, E.; McGrath, J.; Nieminen, T.; Paasonen, P.; Boy, M.; Adamov, A.; Kotiaho, T.; Kulmala, M. Sulfuric acid and OH concentrations in a boreal forest site. *Atmospheric Chemistry and Physics* **2009**, *9* (19), 7435–7448.
- (47) Sipila, M.; Berndt, T.; Petaja, T.; Brus, D.; Vanhanen, J.; Stratmann, F.; Patokoski, J.; Mauldin, R. L.; Hyvarinen, A. P.; Lihavainen, H.; Kulmala, M. The Role of Sulfuric Acid in Atmospheric Nucleation. *Science* **2010**, *327* (5970), 1243–1246.

(48) Wei, G. L.; Li, D. Q.; Zhuo, M. N.; Liao, Y. S.; Xie, Z. Y.; Guo, T. L.; Li, J. J.; Zhang, S. Y.; Liang, Z. Q. Organophosphorus flame retardants and plasticizers: Sources, occurrence, toxicity and human exposure. *Environ. Pollut.* **2015**, *196*, 29–46.

(49) Wendels, S.; Chavez, T.; Bonnet, M.; Salmeia, K. A.; Gaan, S. Recent Developments in Organophosphorus Flame Retardants Containing P-C Bond and Their Applications. *Materials* **2017**, *10* (7), 784.

(50) Sznitman, J. Respiratory microflows in the pulmonary acinus. *J. Biomech.* **2013**, *46* (2), 284–298.

(51) Zaidan, M. A.; Haapasilta, V.; Relan, R.; Paasonen, P.; Kerminen, V. M.; Junninen, H.; Kulmala, M.; Foster, A. S. Exploring non-linear associations between atmospheric new-particle formation and ambient variables: a mutual information approach. *Atmos. Chem. Phys.* **2018**, *18* (17), 12699–12714.

(52) Xu, P.; Kujundzic, E.; Peccia, J.; Schafer, M. P.; Moss, G.; Hernandez, M.; Miller, S. L. Impact of environmental factors on efficacy of upper-room air ultraviolet germicidal irradiation for inactivating airborne mycobacteria. *Environ. Sci. Technol.* **2005**, *39* (24), 9656–9664.

(53) CDC. *Environmental Control for Tuberculosis: Basic Upper-Room Ultraviolet Germicidal Irradiation Guidelines for Healthcare Settings*; 2009. <https://www.cdc.gov/niosh/docs/2009-105/pdfs/2009-105.pdf?id=10.26616/NIOSHPUB2009105> (accessed 2022-02-12).

(54) Vranay, F.; Pirsal, L.; Kacik, R.; Vranayova, Z. Adaptation of HVAC Systems to Reduce the Spread of COVID-19 in Buildings. *Sustainability* **2020**, *12* (23), 9992.

(55) de Souza, S. O.; Cardoso, A.; Sarmento, A. S. C.; d'Errico, F. Effectiveness of a UVC air disinfection system for the HVAC of an ICU. *Eur. Phys. J. Plus* **2022**, *137* (1), 37.

(56) Palakornkitti, P.; Pinyowiwat, P.; Tanrattanakorn, S.; Rajatanavin, N.; Rattanakaemakorn, P. The effectiveness of commercial household ultraviolet C germicidal devices in Thailand. *Sci. Rep.* **2021**, *11* (1), 23859.

(57) Joo, T.; Rivera-Rios, J. C.; Alvarado-Velez, D.; Westgate, S.; Ng, N. L. Formation of Oxidized Gases and Secondary Organic Aerosol from a Commercial Oxidant-Generating Electronic Air Cleaner. *Environ. Sci. Technol. Lett.* **2021**, *8* (8), 691–698.

## Recommended by ACS

### Variations of Wintertime Ambient Volatile Organic Compounds in Beijing, China, from 2015 to 2019

Jing Li, Shaodong Xie, *et al.*

JANUARY 09, 2023  
ENVIRONMENTAL SCIENCE & TECHNOLOGY LETTERS

READ 

### Observed Kinetics of Enterovirus Inactivation by Free Chlorine Are Host Cell-Dependent

Shotaro Torii, Tamar Kohn, *et al.*

JANUARY 17, 2023  
ENVIRONMENTAL SCIENCE & TECHNOLOGY

READ 

### Co-Occurrence of Bromine and Iodine Species in US Drinking Water Sources That Can Impact Disinfection Byproduct Formation

Naushita Sharma, Paul Westerhoff, *et al.*

JANUARY 17, 2023  
ENVIRONMENTAL SCIENCE & TECHNOLOGY

READ 

### Molecular Understanding of the Enhancement in Organic Aerosol Mass at High Relative Humidity

Mihnea Surdu, Imad El Haddad, *et al.*

JANUARY 30, 2023  
ENVIRONMENTAL SCIENCE & TECHNOLOGY

READ 

Get More Suggestions >